J. Fluid Mech. (1969), *vol.* 35, *part* 3, *pp.* 451–479
Printed in Great Britain

The three-dimensional detonation polar and an application to spinning detonation

By A. K. MACPHERSON
Department of Mechanical Engineering, University of Sydney†

(Received 13 December 1967 and in revised form 12 June 1968)

Expressions are derived for a three-dimensional polar in the pressure ratio, deflexion angle space to represent conditions downstream of a detonation wave with given upstream conditions. An analysis of reflected waves is undertaken and the representation of three wave confluences in a three-dimensional hodograph space studied. These techniques are applied to experimental results available for spin detonation in gaseous mixtures of acetylene–oxygen–argon and carbon monoxide–oxygen. Assumptions made in earlier papers concerning local extinction of combustion at the confluence point are not necessary in this picture.

1. Introduction

The shock polar with pressure ratio P/P_0 and deflexion angle (δ) co-ordinates, has been very successful in the analysis of problems involving the confluence of shock waves at a point. A polar, similar to the shock polar, may be developed to represent a detonation wave, by including the heat of combustion q. Thus, using the shock polar and the detonation polar, which is given by Shchelkin & Troshin (1964) as

$$\tan\delta = \frac{P_1/P_0-1}{1+\gamma M_0^2-P_1/P_0}\left[\frac{2M_0^2\left(1-\dfrac{q}{P_1/P_0-1}\right)}{(\gamma+1)\,P_1/P_0+\gamma-1}-1\right]^{\frac{1}{2}},$$

the solution of a confluence involving both shock and detonation waves would be possible. For the few cases for which quantitative results are available upon such mixed confluences, the agreement between experiment and theory has not been as satisfactory as that obtained when only shock waves are present.

Detonation polars were used by Shchelkin & Troshin (1964) to analyze the experimental results on spinning detonation obtained by Voitsekhovsky (1957). It was found, that if the pressure ratios and deflexions across the various waves were calculated, such as to satisfy the wave angles measured by Voitsekhovsky, then continuity of pressure and direction were not satisfied downstream of the confluence. In these calculations the heat of combustion q was taken to be constant at all points on the detonation polars.

Using a varying value of q, which was derived from chemical equilibrium

† Present address: Institute for Aerospace Studies, University of Toronto, Toronto, Ontario, Canada.

calculations, Strehlow (1964) analyzed the results by White (1963) on reactive gas Mach stems. Continuity conditions downstream of the confluence could only be satisfied by assuming that the detonation wave became a shock locally at the confluence point. Similarly, Edwards, Parry & Jones (1966) found that in analyzing their results on spin detonation, the polar for the reflected shock, polar II, figure 1, did not intersect the detonation polar III. Following Strehlow, they assumed that the detonation wave must locally become a shock wave, giving the solution point as G. In the present work, it is suggested that such an assumption of local extinction of combustion, could be due to neglecting the three-dimensional aspects of the problem.

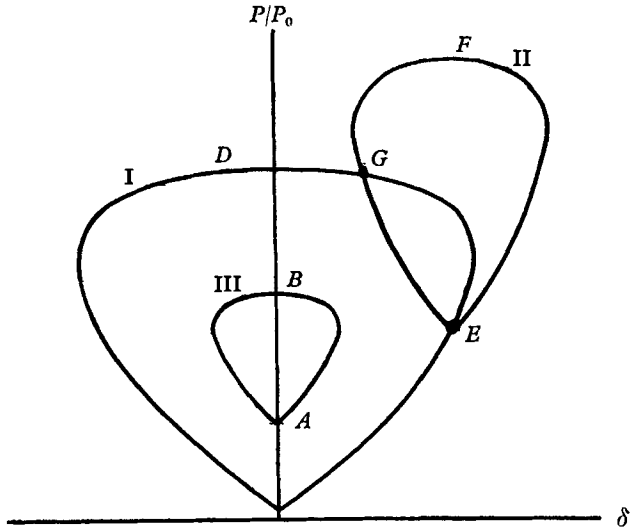

FIGURE 1. Shock and detonation polars for spin detonation from Edwards, Parry & Jones (1966).

Finally, in Macpherson (1968*a*) the results obtained by Schott (1965) on spinning detonation were studied using a two-dimensional polar in which allowance was made for a variation around the polar of both q and γ_1 (the downstream value of the specific heat ratio). Although a solution was obtained, the result was not theoretically satisfying as the resultant wave arrangement did not appear to be generated by any physically reasonable mechanism. A second solution was also presented, assuming that a minimum entropy state was taken up by the dominant driving detonation wave. Although in the minimum entropy case the waves angles did not agree with the measured values, it was assumed that this could be due to three-dimensional effects. Thus a requirement appeared to exist for a polar to represent three-dimensional shock and detonation waves. In the present work, the construction and properties of such a polar are examined together with a discussion of the techniques necessary for its use. This is followed by a description of the application of the technique to some spinning detonation results.

2. The three-dimensional detonation polar

Derivation and properties

The jump conditions across a three-dimensional wave in an inviscid, semi-perfect gas are:

$$\rho_0 u_0 = \rho_1 u_1, \tag{1}$$

$$\rho_0 u_0^2 + P_0 = \rho_1 u_1^2 + P_1, \tag{2}$$

$$\frac{u_0^2}{2} + \frac{\gamma_0}{\gamma_0 - 1}\frac{P_0}{\rho_0} + Q = \frac{u_1^2}{2} + \frac{\gamma_1}{\gamma_1 - 1}\frac{P_1}{\rho_1}, \tag{3}$$

$$\mathbf{u}_0 . \mathbf{v}_i = \mathbf{u}_1 . \mathbf{v}_i \quad (i = 1, 2). \tag{4}$$

Subscripts 0, 1 refer to upstream and downstream conditions respectively. Q, the heat of combustion, is the change in $\sum_{i=1}^{n} (h_i^0(T) - C_{P_i}^0(T)T)$ across the wave where $h^0(T)$ is the standardized enthalpy at temperature T, C_P^0 is the standardized specific heat at constant pressure, n is the number of i chemical species present, $\mathbf{v}_1$, $\mathbf{v}_2$ are independent tangent vectors to the detonation.

A system of axes (l_0, l_1, l_2), preferably right-handed orthogonal, must be defined for the above equations. The system could be chosen arbitrarily, with the result that the incident flow vector would have direction cosines (α, β, γ) and the deflected flow vector direction cosines (l, m, n). Such a selection would have advantages when considering reflected waves; the resultant polar, however, would not have any assured symmetry. A symmetrical polar could be obtained by choosing $\alpha \equiv l_0$, without defining l_1 and l_2. This latter system was selected, as the symmetry property appeared very useful and yet the system retained one degree of freedom.

If the angles δ and ϕ are defined by the relations $\tan\delta = -m/l$ and

$$\tan\phi = -n/l,$$

where δ lies in the (l_0, l_1)-plane and ϕ lies in the (l_0, l_2)-plane, a steady-state detonation polar surface for three-dimensional flow may be obtained from (1)–(4) as

$$\pm[\tan^2\delta + \tan^2\phi]^{\frac{1}{2}} = \pm\frac{P_1/P_0 - 1}{1 + \gamma_0 M_0^2 - P_1/P_0} \times \left[\frac{2\gamma_0 M_0^2}{1+\gamma_1}\left\{1 - \frac{(\gamma_1 - \gamma_0)/(\gamma_0 - 1) + \gamma_0(\gamma_1 - 1)\,q}{P_1/P_0 - 1}\right\}\Big/\left(P_1/P_0 + (\gamma_1 - 1)/(\gamma_1 + 1)\right) - 1\right]^{\frac{1}{2}}, \tag{5}$$

where $q = Q/a_0^2$, a being the speed of sound. As it does not appear that this relation has been previously published, a few brief notes are given in appendix A both upon the derivation of the expression and related properties.

Reflected waves

Consider a three-dimensional confluence such as that of the three waves shown in figure 2 (*a*). As a polar is constructed with the $\mathbf{l}_1$ axis parallel to the incoming flow, the axes $\mathbf{l}_i'$ of polar III for the reflected wave (r), are not parallel to the axes

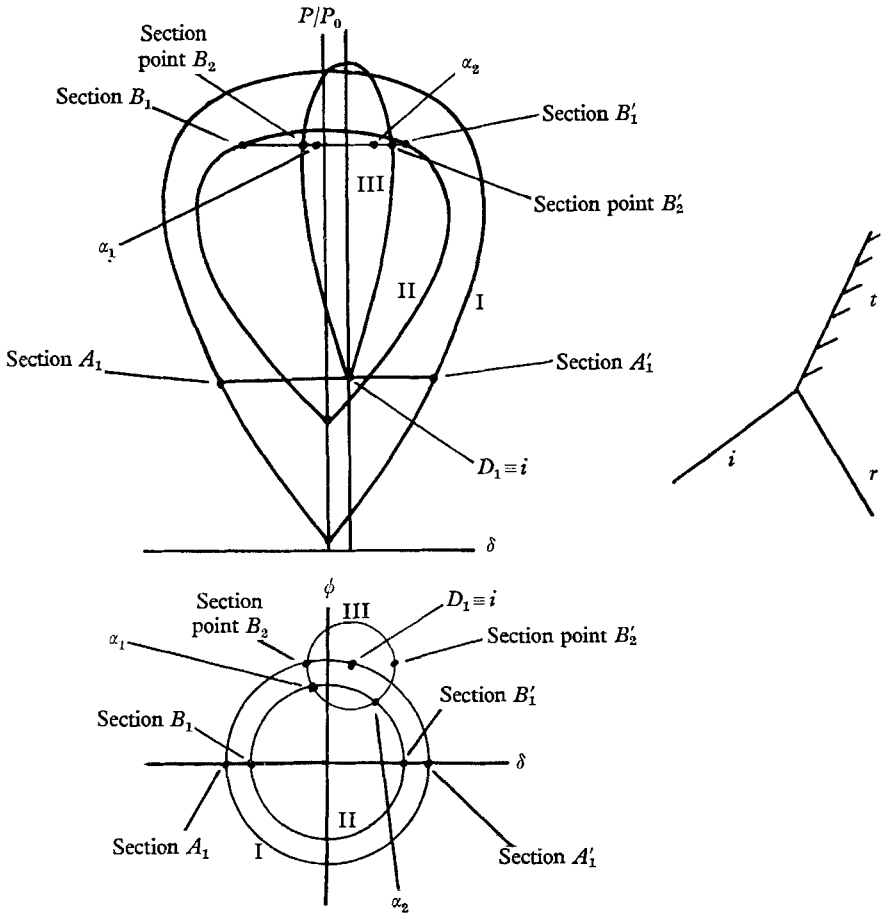

(a)

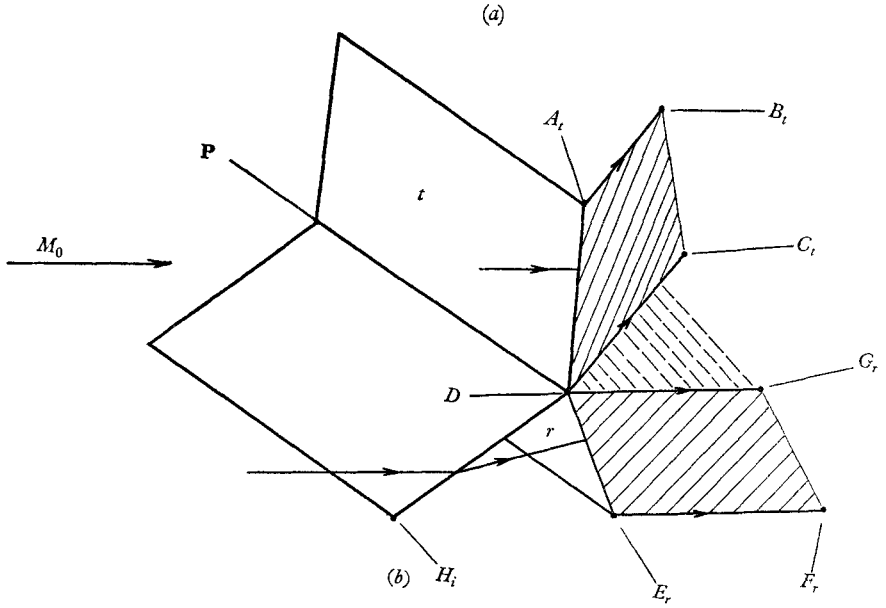

FIGURE 2. Wave confluences. (*a*) Three shock confluence. (*b*) Cross flow three-dimensional shock waves.

$\mathbf{l}_i$ for polar I. Thus, the results obtained for polar III in the system $\mathbf{l}'_i$ must be mapped by rotation as well as displacement for representation in the $\mathbf{l}_i$ of polar I. As the $\mathbf{l}'_i$ axes passes one degree of freedom, a simplification of the rotation matrix may be obtained by choosing $\mathbf{l}'_2$ to be parallel to the (l_1, l_2)-plane. The resultant rotation matrix is given in appendix B. The mapping functions for $\tan\delta'$, $\tan\phi'$ from the l'_i axes to the l_i system become:

$$\tan\delta = (x_0\tan\delta_0 + \tan\delta_0\tan\delta' - \tan\phi_0\tan\phi'(1+x_0^2)^{\frac{1}{2}})/A,$$

$$\tan\phi = (x_0\tan\phi_0 + \tan\phi_0\tan\delta' + \tan\delta_0\tan\phi'(1+x_0^2)^{\frac{1}{2}})/A,$$

where $A = x_0(1 - x_0\tan\delta')$, δ_0, ϕ_0 being the deflexions of the flow behind the incident wave, $x_0 = \tan^2\delta_0 + \tan^2\phi_0$.

As discussed in Macpherson (1968*a*), the deflagration waves can also be mapped by relation (5). Further, a relation for a Prandtl–Meyer wave from a swept corner may be readily obtained in three dimensions from the one-dimensional relations.

One downstream continuity condition for a wave system as in figure 2 is the equivalence of pressure across shear discontinuities. There is also a restriction upon possible flow directions. If the vector $\mathbf{p}$ is defined by the line of intersection of the three wave segments, then the continuity requirement upon the flow directions $\mathbf{u}_r$, $\mathbf{u}_t$ is that the plane formed by $\mathbf{p}.\mathbf{u}_r$ must contain the vector u_t. This condition may most readily be examined by considering the directions of $\mathbf{p}\times u_r$ and $\mathbf{p}\times u_t$, which will be termed condition A. The vector $\mathbf{p}$ is defined in terms of the normals $\mathbf{i}_n$, $\mathbf{t}_n$, $\mathbf{r}_n$, to waves i, t, r respectively as $i_n\times t_n = i_n\times r_n$ and this is termed condition B. Thus for each pressure ratio all waves systems represented by pairs of points on the two polars which satisfy conditions A and B are possible solutions. Thus, as in two-dimensional flow, there are multiple solutions and appeal must be made to boundary conditions to determine the physically likely result in a particular study.

Consider the wave system given in figure 2(*b*). This represents a typical three wave confluence where the edge of the flow downstream of $\mathbf{t}$ and $\mathbf{r}$ are shown as $DA_tB_tC_t$ and $DE_rF_rG_r$ respectively. Thus, for finite length straight waves a boundary must be provided to fill the plane G_rDC_t. As the plane G_rDC_t contains $\mathbf{p}$ it appears difficult to terminate such a system with a smooth boundary unless $DA_tB_tC_t$ is parallel to $DE_rF_rG_r$ and the region C_tDG_r vanishes. This is when $\delta_1 = \delta_2$ and $\phi_1 = \phi_2$ across a shear discontinuity between regions 1 and 2. Further, if the vector $\mathbf{p}$ curves then the region C_tDG_r will contain gas at a different pressure to that downstream of r. This may force the system to become irregular. These considerations will be investigated in subsequent studies. However, as the flow in spin detonation is confined to a small region near the wall it appears reasonable to obtain a first approximation to the wave structure by assuming $\delta_1 = \delta_2$ and $\phi_1 = \phi_2$.

3. Application to spinning detonation results

Acetylene–oxygen–argon mixture

Experimental results

Using heat gauges mounted in the detonation tube wall, Schott (1965) constructed the wave configuration in figure 3 (*a*). The points represent the mean of five tests and it can be seen that although the scatter of points is generally small,

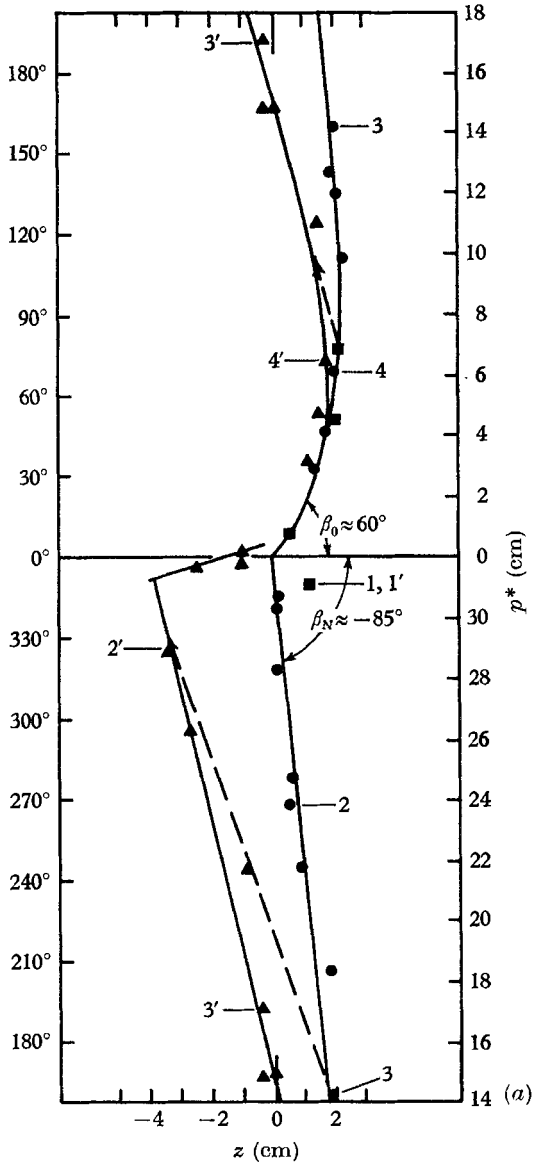

FIGURE 3. Experimental results by Schott (1965) of spin detonation in an acetylene–oxygen–argon mixture. (*a*) Instantaneous axial and circumferential positions of waves dot-shock front, triangle-chemical reaction, square-detonation front. (*b*) Inscriptions in smoked foils on tube walls. (*c*) Definitions of the angles α and β. (*d*) Inscriptions in smoked foil on tube end clear patches are defects on the film.

the point 1, 1′ is particularly astray. A coating of soot placed on the end of the tube, figure 3 (*d*) (plate 1), shows that the effects of the spinning head are restricted to an annular region between 0·65 R and the tube wall, R being the tube radius. The region from 0·73R to the wall is approximately of uniform width. The patterns are only quasi-stable, as shown in table 1 and the related figure 3 (*c*). Soot patterns on the tube walls, figure 3 (*c*), also suggested that the flow was quasi-stable; Schott described these records as 'In the smoothest single spin records α is consistently about 49·5°. The spin pattern is usually not uniform, however, and in a larger number of records α fluctuates between about 41° and 54°. In this fluctuating mode, the track travels a small distance at the lower angle, curves smoothly to the higher one, and later bends abruptly to the lower one. Weak disturbances

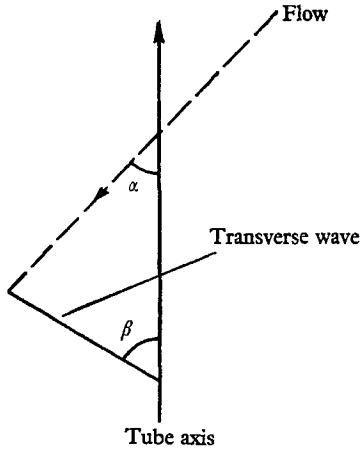

FIGURE 3(*c*). For legend see p. 456.

propagating counter to the dominant helix connect these points of acceleration and deceleration of the circumferential motion. This fluctuation occurs periodically at between 0·60 and 0·67 revolutions. The length of the low-angle track is smaller than that of the high angle.' Thus, for this mixture, the application of steady flow conditions is questionable. As insufficient experimental data was available to choose which of the two modes applied to figure 3 (*a*), average values of velocity and wave propagation angle were used here.

Three-dimensional solutions

In the analysis below the effects of rotation have been assumed to be satisfied in the experimentally observed patterns. Alternatively, the model presented represents spin in a tube of infinite diameter. Further, it has been assumed that the results obtained exist right at the tube wall.

In order to define the different waves referred to in the results, the picture which has been built-up from the calculations, is shown in figure 4. The convention has been adopted that wave boundaries which extend towards the interior of the tube have been shown as tapering curves. The global view of the complete system is shown in figure 4 (*a*), while figures 4 (*b*) to 4 (*d*) give details of the various confluences with appropriate shading to improve definition.

Consider figure 4 (*a*); if the shock at 0° is to be part of a continuous shock across the centre of the tube to 180°, then the shock *i*, figure 4 (*b*), must curve down to the wall from the tube interior near the confluence point at 0°. Hence *t* must also

		Variation			
Quantity	Average	Shot to shot	Over 1 cycle	Over $\frac{1}{2}$ cycle	Local
D, axial velocity, impulse	1·336	± 0·03	± 0·07	± 0·14	—
α, propagation angle	50·0°	± 0·5°	± 1°	± 2°	+ 5° − 8°
β, transverse wave	23°	+ 7°	—	—	+ 9°
Angle	—	− 4°	—	—	− 7°

TABLE 1. Wave velocity and angles deduced from wave-speed photographs (Schott 1965)

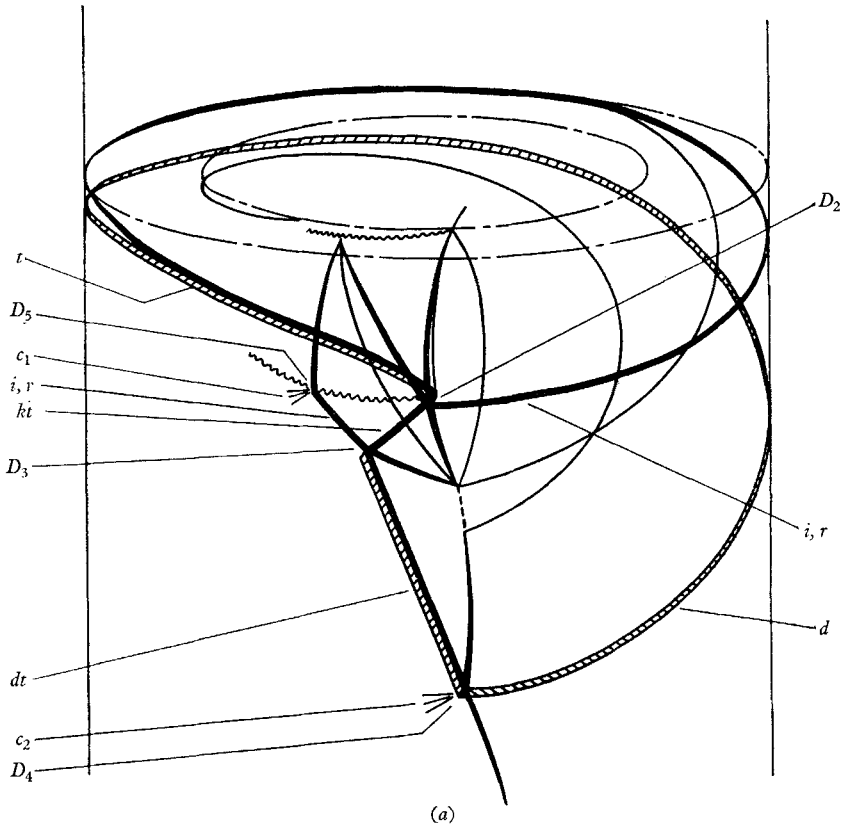

(*a*)

FIGURE 4. Proposed wave structure of spinning detonation.

curve from the tube interior, near the confluence point. Thus, the reflected shock *k* is formed extending into the tube at the junction between *i* and *t*. The experience obtained in the analysis of this three wave group suggests that only the two-dimensional solutions can be obtained, as all others fail to satisfy the re-

strictions upon wave angles at the confluence point. However, it was not felt that a sufficiently detailed study had been made to establish this, although the results were suggestive of a general trend. Further study of such a confluence would require more extensive algebraic manipulation of the equations to reduce computation time for solutions.

As supersonic flow must exist upstream of *dt* the wave *i* must be reflected at the tube wall to form the wave *r*. The boundary conditions imposed on *r* are that the

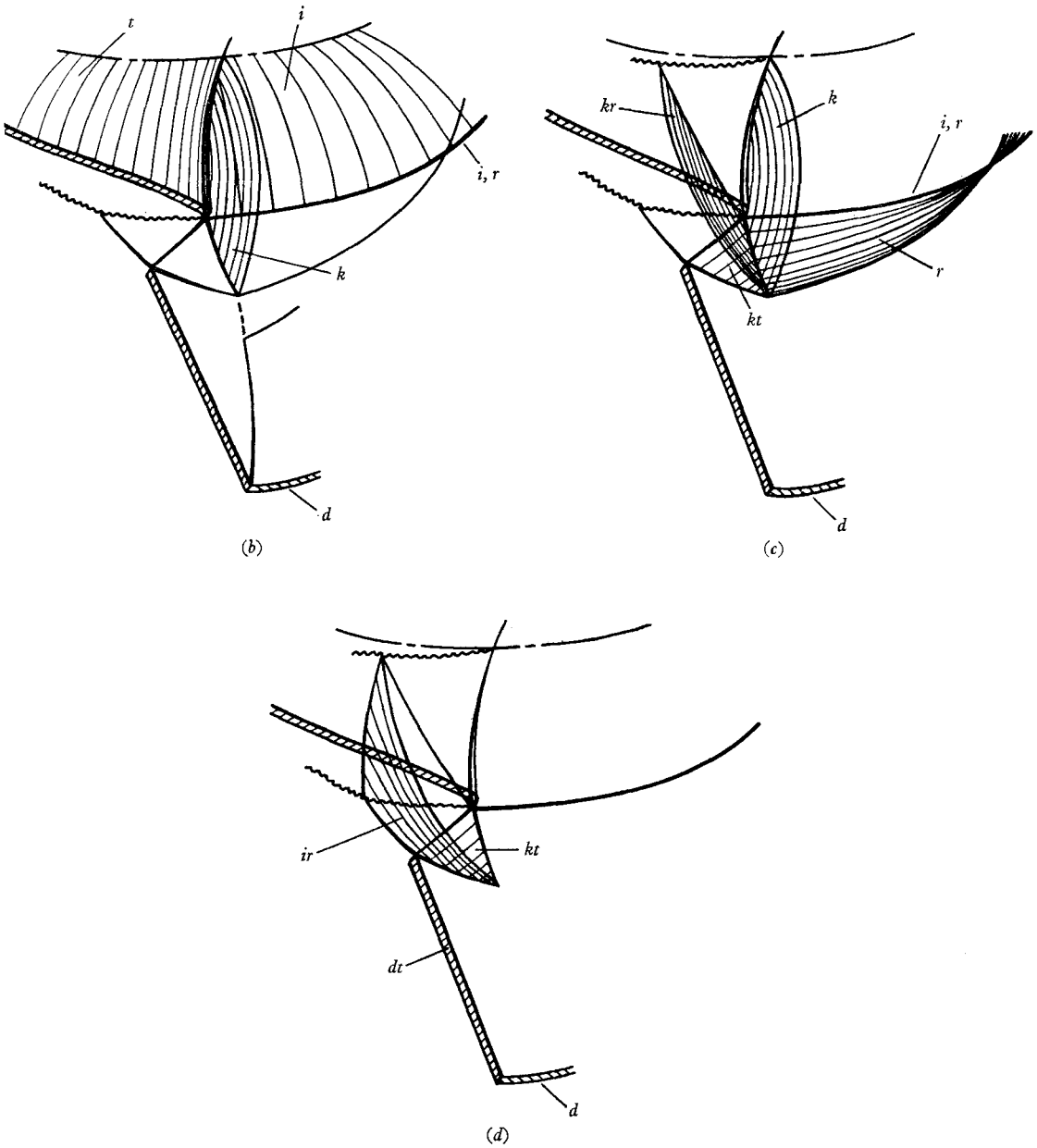

FIGURE 4(*b*)–(*d*). For legend see facing page.

angle θ made by the incident shock at the wall must equal that of the reflected wave, to produce the line i, r in figure 4 (*b*), and that the downstream flow behind r must be supersonic and parallel to the wall. As the $\mathbf{l}_1$ axis in the study was chosen to lie along the radius, the latter condition was satisfied by $\phi = 0$. Thus the procedure used to select r was to calculate the points where $\phi = 0$ at a variety of pressure ratios and then select the one which gave the same value of θ for both the incident and reflected shocks.

Wave	Description
i	Curves from tube centre to meet wall at ir
r	Reflected wave at ir to bring flow parallel to wall
t	Curved detonation from tube centre to wall
k	Triple wave at intersection of i and t
kr	Reflected wave behind k at the intersection of k with r
kt	Reflected wave behind r at the intersection of r with k
dt	Transverse spinning detonation
d	Deflagration wave

TABLE 2. Wave nomenclature

When the wave k meets the wave r, a four wave confluence is most likely formed, figure 4 (*c*). There are many possibilities for this system. The one shown is a four shock confluence with probably a Mach stem between k, kr and r, kt. In studying the four wave confluence it appeared that only a two-dimensional regular confluence is possible when the restriction of equal δ and ϕ is applied. However, as the wave k shrinks to a point at the wall, the possibility arises of involving the more general boundary conditions considered previously. This was not studied, but appeared to represent a likely solution, as the shearing flow would vanish at the wall. From the confluence, the wave kr extends upwards to meet the vortex sheet from the i, t, k junction. As the flow is subsonic behind t in this region, the pressure pulses will be transmitted over the whole area.

Finally, the wave kt will join the transverse detonation dt and the shock ir will be formed, figure 4 (*d*). This meets the vortex sheet along the sonic line in the vicinity of the wall. However, away from the wall, the position is probably not so certain and it has been drawn as not following the sonic line.

No attempt has been made to study the region where the transverse wave dt meets the deflagration, due to the uncertainty concerning the four wave confluence. However, the two-dimensional solution is most likely fairly close. Again, once the upper region is known with certainty, the remainder can be readily found.

Wave refraction

As the incident shock extends into the interior of the tube, the tangential Mach number decreases and hence both the direction of the flow and the incident Mach number decreases. Thus the technique developed by Henderson (1968) for

shock-boundary-layer interaction may be extended to the present case. In this technique, the boundary layer was replaced by thin inviscid layers of gas of slightly differing Mach numbers. The effects of viscous mixing between the streams were ignored. Thus the problem was reduced to one of shock wave

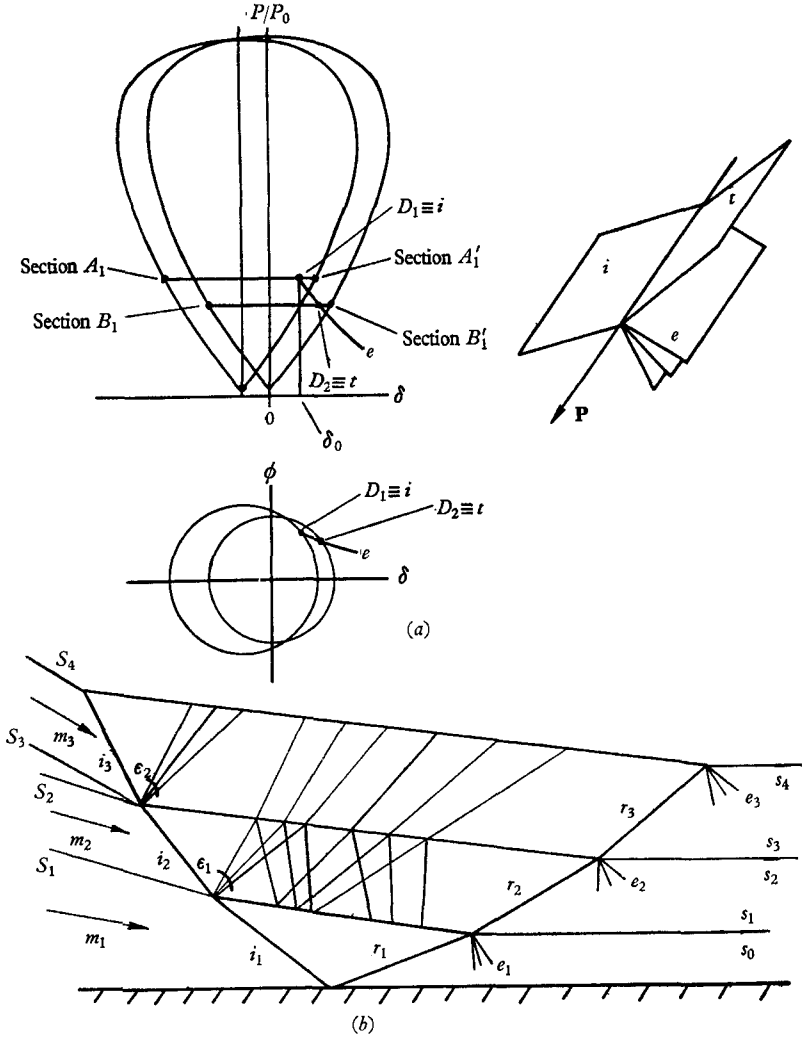

FIGURE 5. Wave confluences. (*a*) Shock refraction. (*b*) Shock reflexion.

refraction. It was found that both types of regular refraction, that is, with reflected shock or reflected expansion, could be obtained. In the present case, the flow may be divided into thin strips of varying Mach number and varying direction, so that the polars for two slightly different Mach numbers are displaced along the axis, figure 5(*a*). Thus again, either a reflected shock or expansion may occur. However, it was determined numerically, that in the range of pressure ratio of interest, the change in δ due to upstream direction change, occurred more rapidly than the change in δ due to decreasing Mach number. Hence, only a reflected expansion is possible.

The refraction of the reflected shock r is far more difficult. Consider the case of of a two-dimensional shock, with upstream Mach number M_i refracted by a negative boundary layer of changing upstream direction, figure 5 (*b*). The incident shock i_2 has a reflected expansion ϵ_1 and a transmitted shock i_1 at the interface S_1S_0. The reflected shock r is produced at the wall. Similarly i_1, ϵ_2, i_2 form a

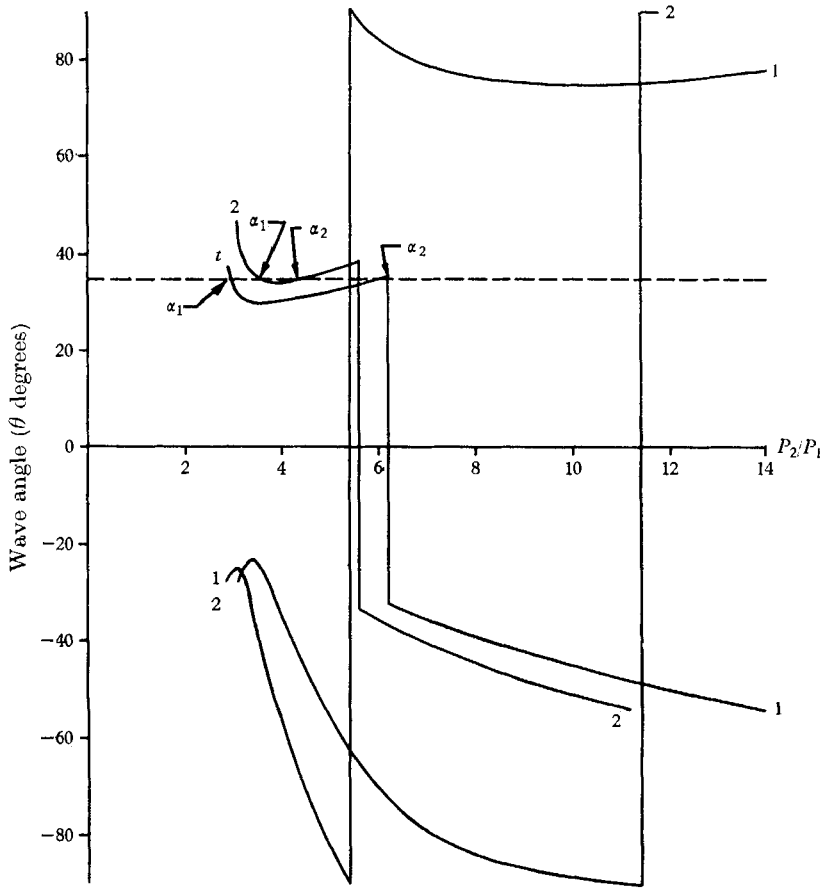

FIGURE 6. Variation with pressure ratio of the wave angle θ, at the tube wall of the reflected wave. Curve 1 $P_1/P_0 = P_L \sim 4{\cdot}7$.

refraction system at the interface S_2S_3. Now when ϵ_1 meets the interface S_2, each wave of the expansion fan will be refracted and a transmitted expansion with a reflected compression wave will be obtained, following Guderley (1962). Again the compression waves will be refracted at the interface S_1. Hence to determine the Mach number and direction upstream of r_2 is very lengthy. The assumption that ϵ_1 is an expansion shock would reduce the computation considerably. However, even with this approximation the cost was beyond the research resources available. Thus, the assumption was made, and it was realized that it was unlikely to be realistic, that all the streams upstream of reflected shock r were parallel to the flow between i_1 and r_1. The Mach number was that behind the

expansion fans e. Under these conditions a reflected expansion e is obtained during the refraction of r, figure 5.

Incident shock selections

If the incident shock-wave angle is fixed at $\theta = +35°$ and the incident shock pressure ratio P_1/P_0 increased from $P_1/P_0 = 1{\cdot}0$ it is found that for $P_1/P_0 < P_L$ only one value of the pressure ratio P_2/P_1 across the reflected shock gave

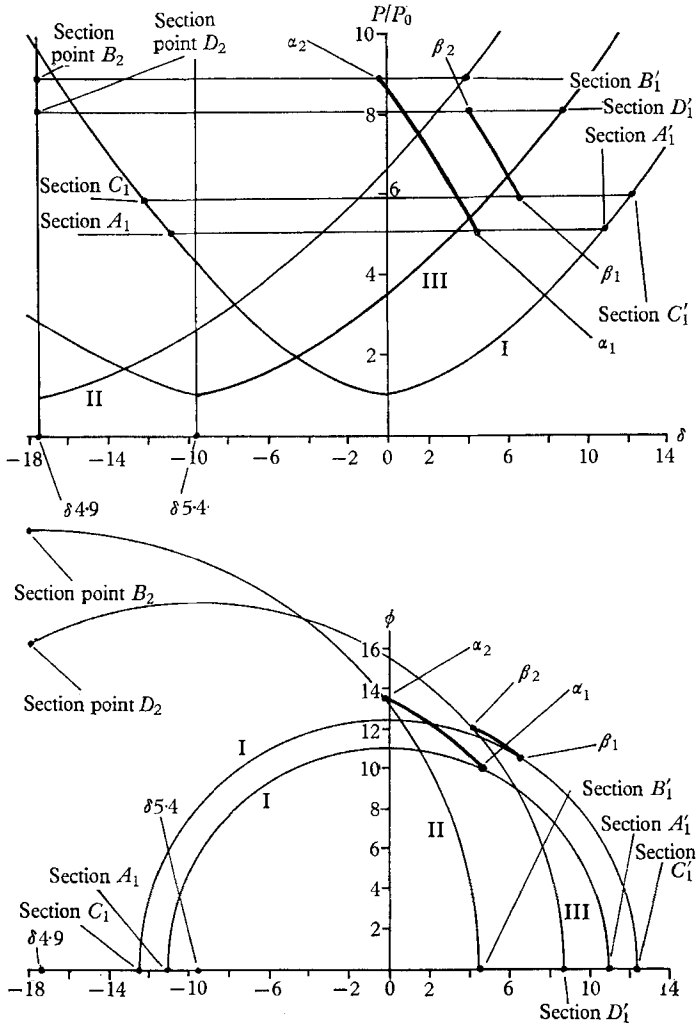

FIGURE 7. Hodograph mapping of refraction of i.

$\theta_r = +35°$. The curve of the variation of P_2/P_1 with θ_r for $P_1/P_0 = P_L$ is shown as curve 1 in figure 6. It can be seen that two values (α_1, α_2) of P_2/P_1 are possible. However, with increasing P_1/P_0 the solutions move together till at $P_1/P_0 = P_\mu$ a double point $\alpha_1 \equiv \alpha_2$ is obtained. This is curve 2 in figure 6. For $P_1/P_0 > P_\mu$ no solutions are possible.

Further, although the mean line for i drawn by Schott, makes 35° with the flow, it can be seen from figure 3(*a*) that the three points near the confluence actually lie on the circumference of the tube, making an angle of 40° with the flow. Away from the confluence the points appear to sweep up quite rapidly.

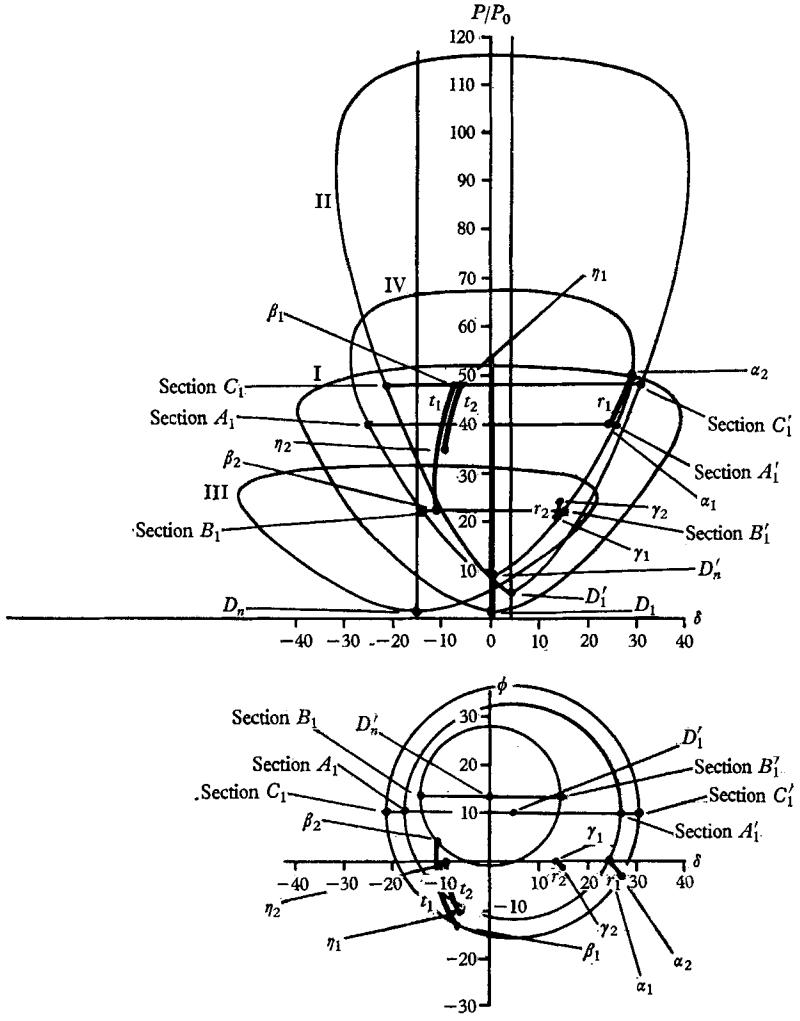

FIGURE 8. Hodograph mapping of refraction of t, k and r.

Thus, a selection principle must be invoked. As for the two-dimensional problem, Macpherson (1968*a*), the entropy change Δs across the transverse detonation dt was used to select the incident and reflected waves. In this case it is the total entropy change across the three-dimensional wave which must be considered. It was found that $P_1/P_0 = P_\mu$ and $\theta_1 \equiv 40°$ (referred to below as the minimum wall entropy solution) gave the minimum entropy at the wall. The use of the 40° solution was attractive as it provided the possibility of double headed spin being developed in the general form suggested by Soloukhin (1966). However, as will be presented elsewhere Macpherson (1968*b*), this does not produce a

physically likely result. The mapping of the wave i in the hodograph plane for this case is shown in figure 7 as the segment from α_1 on polar I to α_2 on polar II. The wave mappings of t, k and r are shown in figure 8, as the segments β_1 to β_2 for k, t and α_1 to α_2 for r. Thus, it was decided to develop an α_1 solution with $\theta = 35°$. The results of this analysis are given below.

Development of an α_1 solution

As some results had already been produced for an incident shock i with pressure ratio 5·88 prior to the realization of the possible importance of entropy change across dt, this solution was completed. In this case, the waves k and t were only obtained at a few points, as the behaviour of these waves appeared from the previous results to be quite regular. Further, the calculations were terminated shortly after the transverse detonation dt ceased to exist.

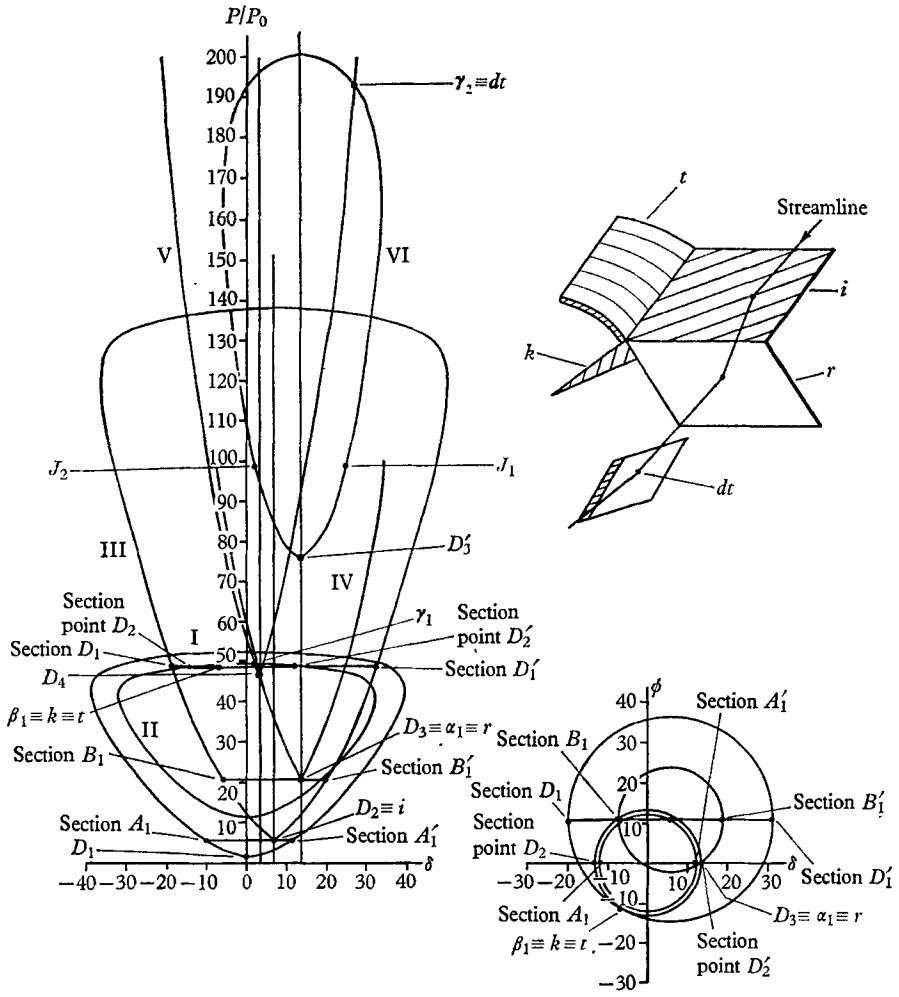

FIGURE 9. Hodograph mapping of i, r, t, k and two-dimensional solution for kt, kr, dt (α_1 solution).

Figure 9 shows the mapping of the wave i as D_2 on polar I, the reflected wave r as D_3 on polar III and k, t at β, as the intersection of polars I and III. No attempt has been made to analyze the four waves confluence at k, v, kt, kv, figure 4(*c*). However, a two-dimensional solution has been constructed for the wave kt at the wall. The solution γ_1 is obtained on polar IV constructed at D_3 and the wave ir is given by γ_2 on polar V constructed at D_4. Thus, γ_2 should be close to dt on polar VI. This may now be compared with the experimental measurements of β_1 the transverse wave angle in table 1. The wave angle θ of dt with respect to the flow direction $\delta = 13{\cdot}5°$ behind r should be $86{\cdot}5°$, whereas the two-dimensional solution at γ_2 gives the value of $\theta = 80{\cdot}8°$. However, the value of $\theta = 80{\cdot}8°$ would only apply right at the confluence point, whereas β_1 is the most likely average value, probably close to J_1 where $\theta = 61{\cdot}8°$. It was found that the transverse wave dt could exist till the Mach number on the wave i was reduced to 5·6. The polars at $M_1 = 5{\cdot}6$ were constructed where polar I contains i, polar II contains r and polar III represents dt. It was found that the Chapman–Jouguet points coincide at the base of the polar III and all points on the polar are thermodynamically possible.

Table 3, a copy of which can be obtained from the editor, contains the results of the refraction, where the deflexions are given in the co-ordinates of the wave considered, δ_0, ϕ_0 and the co-ordinates of the shock i at the wall δ_{rl}, ϕ_{rl}. The wave angles θ_{rl}, ω_{rt} are given in terms of a co-ordinate system with axis l_1 along the radius and l_2 parallel to the tube genetarix. The third angle is the intersection of the wave with the (l_1, l_2)-plane. The temperature T is downstream of the wave. The values for δ_1, ϕ_1 are plotted in figure 7 as the segment β_1, β_2 for i and in figure 8 as η_1 η_2 and γ_1 γ_2 for the waves t, k and r respectively. The results follow the minimum wall entropy solution very closely except for the reflected wave r. In fact, this wave barely alters and at γ_1 has a pressure ratio very close to that of a normal $M_1 = 4{\cdot}12$ shock. The most significant difference is in the temperature downstream of the wave r. In the minimum wall entropy case, a temperature about 1600 °K was found downstream of r, and hence combustion is likely. In this case combustion is very unlikely to occur, as the approximate minimum for combustion from the work by Kistiakowsky (Glass, Kistiakowsky & Michael 1965) is 1400 °K. The temperature gradient between the flow downstream of k and behind t is, however, in the temperature region where combustion will occur.

Carbon monoxide–oxygen

Experimental results were obtained by Mitrofanov, Subbotin & Topchian (1963) on spin detonation in a mixture of $2CO + O_2 + 3\,\%\ H_2$. The tube was 27 mm diameter, an initial pressure of 0·1 atm, axial velocity 1700 m/sec and propagation angle $(\frac{1}{2}\pi - \alpha) = 34{\cdot}5°$. The angle α is the angle between the flow direction relative to the spinning head and the tube genetrix.

The axial Mach number was calculated as 4·82 and the helical Mach number as 6·8. The diagrams in the original paper were not available and figure 3 shows the results as given by Oppenheim (1965). The pressure gauges used were polarized barium titanate, calibrated by shock waves of known strength. The author has not used these gauges so that the following comments could be influenced by a

lack of knowledge of the characteristics of the gauges. However, Bernstein (1961) found that with use, the polarization decreased and the gauges became inaccurate. This particularly occurred when the gauges were exposed to elevated temperatures.

As was shown previously (Macpherson 1968*a*) the mass fraction of H_2 present is very important in the evaluation of q. Thus, the quantity of water vapour present is an important factor. In the report upon these experiments, neither the method of preparation nor the technique used to dry the gaseous mixture are given. Thus it has been assumed that the mixture is perfectly dry. Upstream temperatures have not been given and have been assumed as 300 °K. Both these assumptions could have an influence upon the results. Further, the axial velocity and helical angle were not determined at the same time as the experiments, and hence the possibility of different moisture contents being present occurs. Finally, the velocity given suggests that the value has been taken to the nearest hundred m/sec. This is reasonable as Schott found a variation of 70 m/sec over the cycle. However, the variation in this case has not been given, nor is it indicated whether the average lies above or below 1700 m/sec. As will be seen, this is very important. The results by Mitrofanov *et al.* (1963) are given in figure 10 (plate 3).

Numerical calculations

As both the angle of i and the pressure ratio across i, r were known, the point D_3, figure 11, could be readily found using similar techniques as described previously. It was found that this required the α_1 solution. Thus the waves k, t at the wall were found and mapped as β_1, a point with $\phi = 0$. Again, the $\phi = 0$ solution was constructed for dt. It was found that the intersection between polar V for ir and polar VI for dt occurred at a pressure ratio in excess of 200. This result was obviously not observed in the experiment. However, the Chapman–Jouguet pressure ratio on polar VI is 125 which is fairly close to that observed in frame 6.

When the refraction of i was considered, it was found that the axial Mach number of 4·82 produced a detonation wave. Thus, combustion would be expected to extend across the whole tube, which was not in accord with experiment. As the axial velocity did not appear to be known accurately, it was decided, for the purpose of calculating the change in direction of the incident flow across the tube, to assume an axial velocity of 1600 m/sec or $M = 4{\cdot}5$. This was more in accord with the results of acetylene. An examination of the results obtained by Bone, Fraser & Wheeler (1936) indicates that a similar situation for a moist CO, O_2, H_2 at atmospheric pressure exists. This suggests that some factor has been ignored in these calculations. One possibility is that the temperature at the Chapman–Jouguet point does not cause combustion as discussed in Macpherson (1968*a*). However, in neither case is the error large, nor are the axial velocity and upstream conditions stated accurately.

Table 4, a copy of which can be obtained from the editor, shows the results of the application of the numerical techniques previously described. The hodograph mapping of i is shown in a similar fashion as previously in figure 12. The wall position is indicated by α_1 and the final value at $M_1 = 5{\cdot}1$ as α_1. The refraction of

i was terminated at this value, as the assumption made for the axial Mach number was beginning to play a dominant role. Figure 13 shows the mapping of k, t from β_1 to β_2 and of r from α_1 to α_2. In this case the position of the final shock

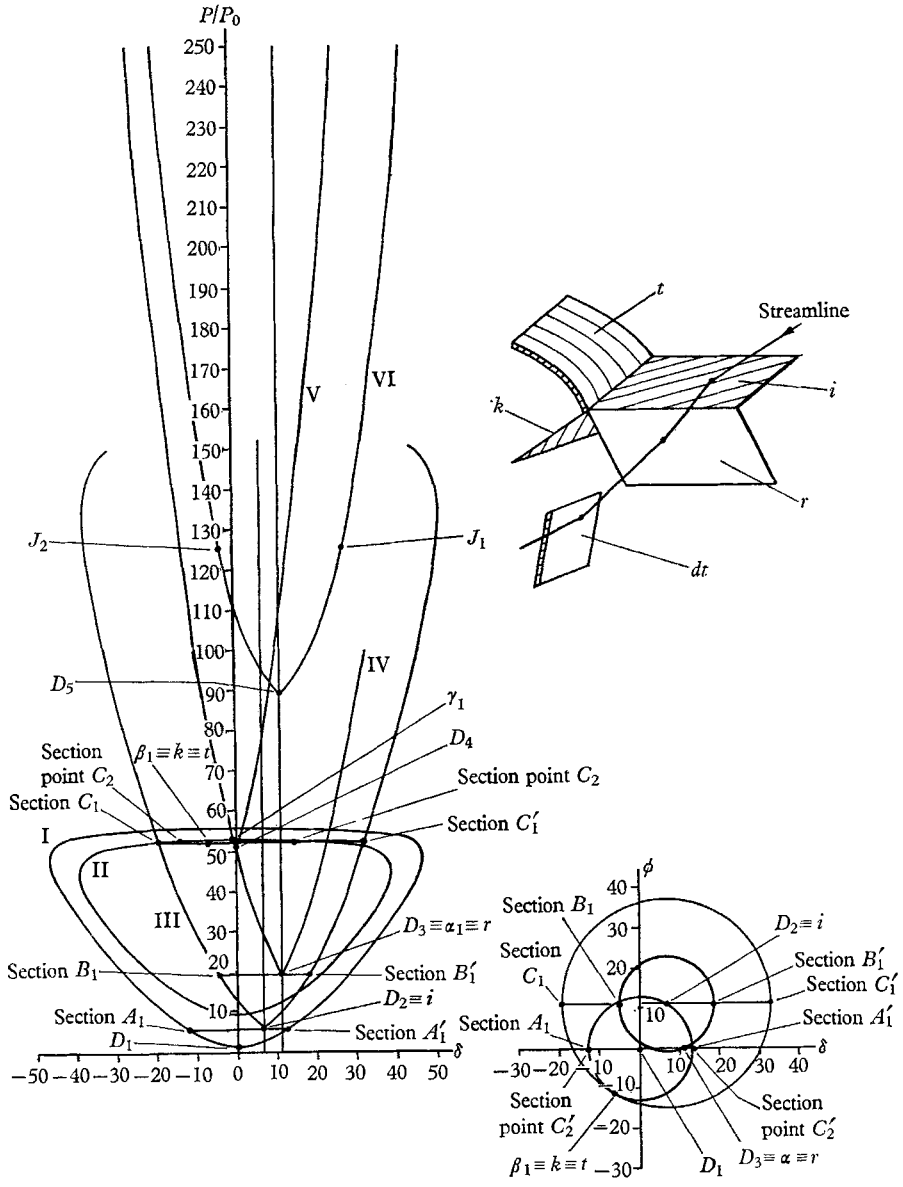

FIGURE 11. Hodograph mapping of waves i, r, k, t and two-dimensional solution for kt, kr, dt.

polars have been indicated by the value of δ_0 for the incident shock i. It was found that dt could not exist for an incident Mach number much less than 5·6 and the corresponding detonation polar is shown in figure 13 as polar III. The pressure ratio across a normal $M = 4{\cdot}82$ shock is $\sim 28{\cdot}5$ so that points β_2 and α_2 are both

well placed to join with such a wave at the centre core of the flow. The value of $\phi = 5{\cdot}5°$ for k, t is well within the expected error. The whole result in this case is very similar to that obtained for the solution in the acetylene mixture.

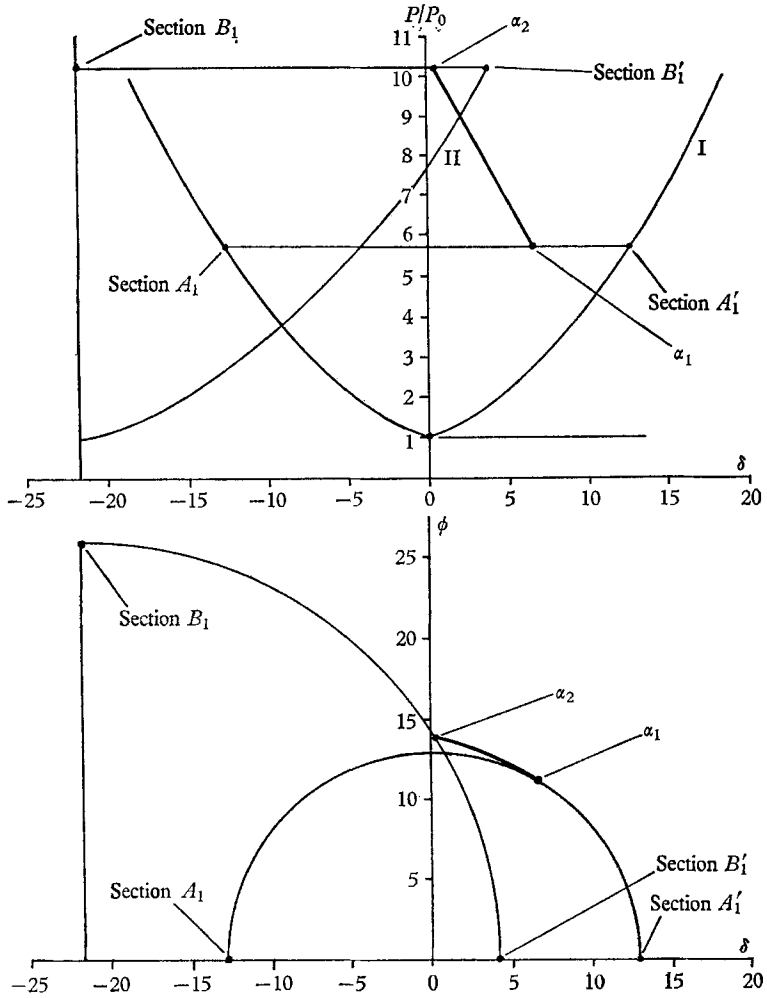

FIGURE 12. Hodograph mapping of refraction of i.

Discussion of experimental results

The shock preceding Chapman–Jouguet detonations has $P/P_0 = 26{\cdot}9$ and the C–J detonation as $P/P_0 \sim 15{\cdot}0$. Thus, the present calculations would suggest that frame 3 was close to the Chapman–Jouguet point. If this is true then frame 4 should contain the deflagration. It is rather disturbing that a constant pressure plateau is not found between the shock and the Chapman–Jouguet deflagration pressure ratio of 10. This suggests both that a constant chemical composition region does not exist and that the representation of the deflagration as a gas discontinuity is rather poor.

The interpretation of frame 5, that the shock is due to the confluence of the deflagration and the transverse detonation, does not accord with the present calculations. From the analysis of the acetylene mixture, a pressure ratio across

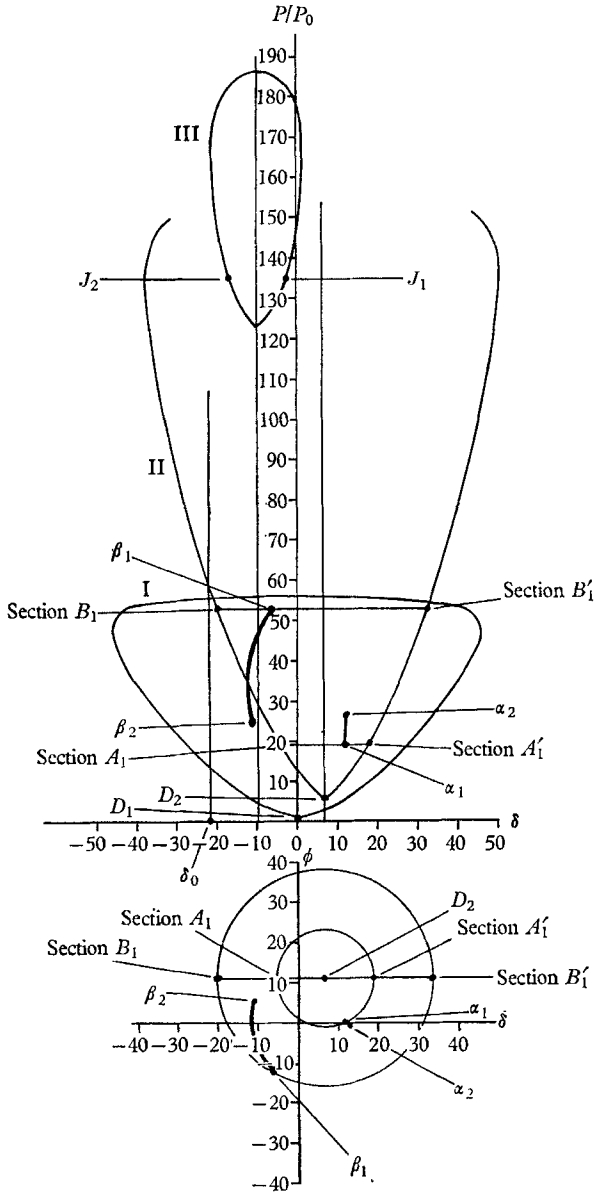

FIGURE 13. Hodograph mapping of refraction of k, t, r.

the shock of about 50 would be expected,† whereas the value obtained is over 75. With the present model, this result is not explained, as the lower confluence was only studied in two dimensions. It was suggested above that neither the trans-

† Due to the polars for the two mixtures being approximately the same, the C_2H_2 results should give a guide as to the expected values for CO.

verse detonation nor the deflagration may be normal to the wall; thus the other waves at the confluence would have reflected shocks at the wall. This could increase the pressure ratio.

It appears reasonable that frames 6, 7 and 8 can be interpreted as in figure 4. These form the basis for the present investigation as the pressure ratio across i and r is obtained as $\sim 19{\cdot}4$. Considerable effort was spent in attempting to fit an alternative interpretation to these results. However, with the given pressure ratios and the time interval between the two waves, it was found that an alternative wave confluence could not be found.

It seems likely that frame 9 agrees with the present work. However, frames 10 and 11 are not considered to be reliable. This particularly applies to frame 11, where a pressure rise of 50 is obtained instantaneously. In frames 6–8, a constant rise time of about 1 μsec is seen for all the waves. Thus in 11, a very strong shock with pressure ratio in excess of 200 would be needed to cause such a rise. It is suggested that the effect of elevated temperatures may have affected the results. Due to irregular pressure changes frame 12 appears too confused for interpretation with the present results.

4. Errors in the numerical model

Before discussing the results generally, a few comments upon the assumptions made in the present study are presented.

The most important assumption is the neglect of rotational effects and particularly the failure to consider the moment of momentum relation. This is simply the cross-product of the radius vector and the momentum equation. As the momentum equation is satisfied across the shocks, locally the moment of momentum will be satisfied. A numerical integration would be required to examine whether the global equation was also satisfied.

Centrifugal and other rotational problems, particularly between waves i and r could only be examined by numerical solution of the flow equations in three dimensions and including conservation of angular momentum. This presents a formidable task, particularly as previous experience suggests this would be an extremely costly venture. As stated previously, it seems reasonable to assume that these conditions have been satisfied in the experimentally observed model. However, the flow between waves i and r is only very approximately defined without a complete solution. The fact that the spin rate is not greatly affected by either tube diameter or shape, suggests that the rotational effects may not be dominant in the solution.

Another important assumption is that the inviscid flow shock waves exist right to the wall. It can be shown by even a crude dimensionless analysis based upon Lighthill (1956), that the curvature of the shock at the shock tube wall is of the order of a few mean free paths. Thus the leading waves i, t will exist for all practical purposes at the wall. The remaining waves, however, will encounter a negative boundary layer set up by i, t. The experimental data upon such boundary-layer growth appears fairly sparse, although such experimental results as Gooderum (1958) tend to indicate that the boundary layer will be less than 0·05 in.

at the tip of the transverse wave. Nevertheless, this thickness will have some effect upon the pressure, temperatures and wave position.

Viscous effects will also be important where a number of shocks meet at a point. When a wave is a detonation and meets at a confluence, the effects of viscosity are unknown. Heat transfer effects will be very important between the flow behind t and that behind k; in fact, at the boundary, it would be very unusual if locally combustion did not occur due to the large temperature gradient.

Finally, it would appear from the pressure profiles obtained by Mitrofanov *et al.* that a constant composition region does not exist behind i, r and that the deflagration cannot be well represented by a gas discontinuity. The main hope in this case is that, although the local effects may be important, the global significance could be slight. Thus, generally, the present model is as firmly based as knowledge of experimental results and computer limitations will permit.

5. Discussion and significance of numerical results

For refraction of a shock wave by a boundary layer, Henderson (1968) showed that the system becomes irregular near the wall and a lambda foot is formed. Thus, at the outset of the present study, it was thought that an irregular wave pattern would be formed after the refraction had proceeded for some distance from the wall. One possibility would be when the polar for wave k failed to intersect the polar for t. As has been shown, this does not occur till shortly before t vanishes and is thus unlikely to have significant influence upon wave structure. The wave system is remarkable in the regularity of the principle waves i, r, t and k, for all conditions considered. The only significant point is that the wave r goes to the sonic point in the minimum wall entropy case for C_2H_2. However, neither of the other two cases show this tendency. In addition, as the $CO + O_2$ results have defined the waves i, r at the wall uniquely, it would be expected that these results would be more significant than C_2H_2 predictions. Thus the minimum wall entropy refraction of r tending to the sonic point may not be the physically observed result.

If i is considered to be refracted to the centre of the tube, it almost certainly would form an irregular pattern as the upstream flow direction would change very rapidly to reach $\frac{1}{2}\pi$ at the centre. The refraction of i much past the point where all detonation becomes impossible appears meaningless, as the driving-piston will be absent. The disturbances which do exist past this point will be rapidly dissipated by viscous forces.

Hence the view of a smoothly curving wave i meeting a flat centre section emerges. If the tangential velocity component varied linearly from its value at the wall to zero at the centre and the wave angle λ_{rt} plotted against tube radius, curve 1, figure 14(a) is obtained for the minimum wall entropy C_2H_2 case. Also shown on this figure, as curve 2, is the highest point on the waves i, t, which would represent the centre section of the shock. As curve 1 does not intersect 2, a linear velocity distribution was found which could allow the wave i to intersect curve 2. This is designated curve 3. It can be seen that the wave i extends to $0{\cdot}63R$. Using the same velocity distribution which allowed curves 2 and 3 to intersect,

the values of λ_{rt} for the α_1 solution in C_2H_2 were plotted in figure 14(*b*). In this case, the wave does not reach curve 2 as the wave was not refracted till all detonation became impossible. However, the transverse detonation ceased at $0{\cdot}73R$. These values may be compared with the results obtained from the soot patterns on the end of the tube shown in figure 3(*d*). There the constant width section extended to $0{\cdot}7R$ and the complete trace vanished at $0{\cdot}65R$. Thus the interpretation may be made that the constant width section represents the region where a transverse detonation exists, and the tapered section where only the wave *t* is present.

No such comparison can be made with the results by Mitrofanov *et al.*, as the position of the waves *i*, *t*, depends upon the interpretation of separate pressure readings. Thus the height of the centre plateau is not defined. However, it can

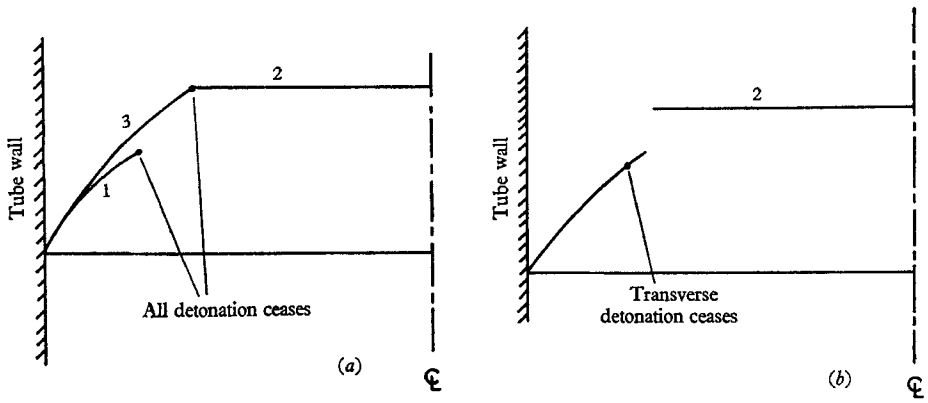

FIGURE 14. Slope of the incident shock *i* along the tube radius from the tube wall.

be seen from a comparison between the values of λ_{rt} for C_2H_2 and CO mixtures, that a similar result may occur. However, further experimental results are required upon this aspect.

It appears likely that the α_1 solution will generally be the most likely one to be obtained in an experiment. There are a number of reasons for this conclusion. The fact that this solution was defined by the results in the $CO + O_2$ mixture is significant, although this could be restricted to the particular mixture. However, the temperature behind the reflected wave *r* became very high when the α_2 solution was considered in the acetylene mixture. For this mixture, recent work by Homer & Kistiakowsky (1967), suggests that at 1800 °K considerable chemical reaction occurs. Further, in the $CO + O_2$ mixture the temperature downstream of *r* is kept low by considering the α_1 solution, although even at these temperatures the experimental results suggest a continuous chemical change. Again, it has been found from studies upon the confluence of shock waves that, if the solution is multi-valued, then the weakest solution will occur in the absence of downstream boundary conditions. This suggests the selection of the α_1 solution, as a smaller entropy change occurs across *r* for the α_1 solution. Finally, the minimum entropy change concept probably required the solution. Unfortunately, the calculations performed were insufficient to either confirm or refute this suggested selection

principle. In fact the whole flow would have to be solved for a number of different conditions to obtain sufficient data.

Consider conditions as the waves meet the centre shock. Provided the α_1 solution is chosen t, k and r have pressure ratios of the same order as the normal shock with the axial Mach number. Further, $\phi \sim 0$ for these waves, which is all that is necessary, as differences in δ between a wave and the normal shock core merely produce a shear layer. Small differences from the centre conditions could be adjusted by a cylindrical shock. The existence of such a shock is also suggested by the fact that there is no trace in the flame pictures of the combustion separating into a deflagration wave behind the wave *dt*. The transverse detonation is clean cut and as pointed out by Schott, in the acetylene mixture, even the difference in wave width due to the rotating head moving either in the same direction as or opposite to the film direction can be seen. If the wave *dt* was not terminated suddenly, such as by a shock, a separation of the deflagration would be expected.

A possibly related feature is that between the waves i and *dt* there exists a supersonic rotating flow. Now the characteristics of such a flow could coalesce into a cylindrical shock. It is possible that this shock, if it exists, could be the same as the terminating shock discussed above. In such a case this wave could be one of the most important in the confluence.

If the centre shock is an almost plane normal wave as suggested here, then all downstream disturbance may propagate up the centre core to influence the whole wave system. Thus disturbances in the subsonic patch behind t could move along the radius and influence all waves through the core. Hence the mode of operation of the tuned oscillator referred to in the literature is apparent. This would tend to support the theory by Fay (1952) of acoustic vibration in the tube. However, it appears that many other influences affect the confluences as well.

As discussed in Macpherson (1968*a*) an explanation of the soot patterns obtained upon the tube walls requires a much better knowledge than is at present available, of the effects of different wave processes upon the soot. However, one feature that appears to be often overlooked is that a soot pattern is not a snapshot but contains traces due to all disturbances which pass the given point. Thus the fine lines found in some soot patterns of spin detonation need not arise from the region between r and the deflagration. The regularity of these waves suggest Mach lines. It was thought that as the waves i, r virtually represent a Mach reflexion, then the characteristics may be inscribed by this wave sweeping across the soot. However, the angles obtained would be 32° and 80° whereas the measured values were 20° and 75°. For these angles to be produced by characteristics, the flow Mach number would be about 2·2. Such a value is only likely to be found behind the shock formed by the confluence of *dt* and the deflagration *d*.

The two different modes found from the soot track, figure 3, have a number of possible explanations. The smooth change at one extreme suggests that in some part of the wave structure, the deflagration which forms part of a detonation slowly moves away from the shock. The wave structure is then altered so that a wave that was previously a shock has an increased temperature downstream and, after a short delay, it explosively forms a detonation giving a sudden change in wave structure. Such an event could occur at waves *k*, *kr*, *ir*, *kt* when, if one of

these became a detonation, the incident wave angle of i could change from $\theta = 35°$ to $\theta = 40°$ say. Alternatively, the change could cause r to move from the α_1 to the α_2 solution.

One of the most disturbing features of the present calculations is that the analysis indicates that detonation would occur across the whole tube for the CO mixture, whereas for the C_2H_2 mixture there is a reasonable margin between the minimum detonation Mach number and the axial Mach number. From flame photographs, such as those by Bone, the striations are clearly defined and hence combustion does not occur in the centre. The only suggestion which can be put forward is that the temperature achieved is insufficient to cause ignition and commence the chemical reaction. This is not very satisfactory and it appears that further research is required upon this point.

Finally, although the wave *dt* has not been studied in detail, the indications are that it is not a two-dimensional wave normal to the wall. This is due not only to the angle at the Chapman–Jouguet point being considerably different from the observed value, but it does not appear that $\theta = 0$ for *kt*. Further, the pressure ratio obtained in the case of $CO + O_2$ is very much higher than the experimentally observed value. This would be modified if a three-dimensional solution was considered.

6. Concluding remarks

A three-dimensional picture has been constructed for some of the main waves in the spinning mode of detonation. Possible shapes of some experimentally observed waves have been predicted. In addition, a number of waves, which have not been observed experimentally, have been predicted. It seems profitable then to list possible avenues for further experimental and theoretical studies, which the present investigation has revealed.

A most important experiment would be the determination of whether the wave r, the reflexion of the incident shock i at the wall exists. This would appear to present a fairly difficult exercise using conventional Schlieren techniques. The pressure ratios and the inclinations of the wave i, r should also be determined for a number of different gases to confirm that the α_1 solution is always obtained. At the same time, the change of mode in observed soot patterns may be revealed.

A determination of the distance which the transverse detonation *dt* extends across the tube is needed. It would seem that this could be readily obtained by using a series of annular masks at different radii on the end of the tube in a similar fashion to that used by Campbell & Woodhead (1928). Further, the presumed existence of a flat normal shock across the centre of the tube requires investigation. This appears to provide a considerable problem experimentally. At the same time, it may be possible to determine if the centre shock rotates as a whole, although this seems unlikely. The suggested cylindrical shock at the junction of the flat shock and the incident shock i may be detected, although this could be very difficult.

Experimentally, it appears unlikely that the four wave confluence *k*, *kr*, *kt*, *r* can be examined, but a theoretical study would be very useful. Considerable

effort would be required in such an analysis, as a preliminary examination of the necessary restrictions of the continuity of the deflexion angles at the junction is needed. However, this type of shock confluence has applications in other fields; for example, at the raked tip of a supersonic aerofoil in three-dimensional flow.

Further theoretical work is necessary on the nature of the lower confluence between the transverse detonation *dt* and the deflagration *d*. However, no progress can be made here, until the four wave confluence mentioned above is solved. It seems unlikely that both *dt* and *d* will be normal to the wall.

An improved method for calculating the refraction of the reflected wave *r* is necessary for theoretical studies both in the present field and for shock-boundary-layer interactions, Henderson (1968). Finally, the possible focusing of the characteristics of supersonic rotating flow in the region *i–d* could produce a shock wave. Were this to occur, it could provide a boundary condition upon the radial extend of the spinning detonation.

Appendix A. Derivation of the detonation polar

Consider a shock wave with angles θ and ω as shown in figure 15. Manipulating the relations in (1) both the Hugoniot relation

$$P_1/P_0 = -\frac{\dfrac{\rho_0}{\rho_1}\dfrac{\gamma_0+1}{\gamma_0-1}+\dfrac{2q\gamma_0}{a_0^2}}{\dfrac{\gamma_1+1}{\gamma-1}\dfrac{\rho_0}{\rho_1}-1} \tag{A 1}$$

and the Rayleigh line expression

$$\gamma_0 \mathbf{M}_0^2 . \mathbf{n} = \frac{P/P_0 - 1}{1-\rho_0/\rho_1} \tag{A 2}$$

may be obtained. With n the normal to the shock, and direction cosines

$$\tan\theta\tan\omega/x, \quad \tan\omega/x,$$

and $$\tan\theta/x, \quad x = [\tan^2\omega + \tan^2\theta(1+\tan^2\omega)]^{\frac{1}{2}}$$

combining the relations yields

$$1+\frac{1}{\tan^2\theta}+\frac{1}{\tan^2\omega} = 2\gamma_0 M_0^2 \frac{\dfrac{P_1/P_0}{\gamma_1-1}-\dfrac{1}{\gamma_0-1}-\gamma_0 q}{(P_1/P_0)\left(\dfrac{\gamma_1+1}{\gamma_1-1}\dfrac{P_1}{P_0}+1\right)} = D. \tag{A 3}$$

The direction cosines of the flow vector downstream of the shock (figure 16) are

$$\left(\frac{-1}{(1+x^2)^{\frac{1}{2}}}, \quad \frac{\tan\delta}{(1+x^2)^{\frac{1}{2}}}, \quad \frac{\tan\phi}{(1+x^2)^{\frac{1}{2}}}\right)$$

where $x^2 = \tan^2\delta + \tan^2\phi$. Using continuity of mass across the shock it may be shown

$$\frac{\rho_2}{\rho_1} = \frac{1+\tan\theta\tan\delta}{1-\dfrac{\tan\delta}{\tan\theta}-\dfrac{\tan\phi}{\tan\omega}}. \tag{A 4}$$

From continuity of tangential components of velocity

$$\tan\theta\tan\delta = \tan\omega\tan\phi. \tag{A 5}$$

Equations (A 3) and (A 5) give

$$\tan^2\theta = \frac{\tan^2\theta\phi + \tan^2\delta}{(D-1)\tan^2\delta}. \tag{A 6}$$

Combining (A 1), (A 4), (A 5) and (A 6) the polar expression may be obtained after considerable manipulation.

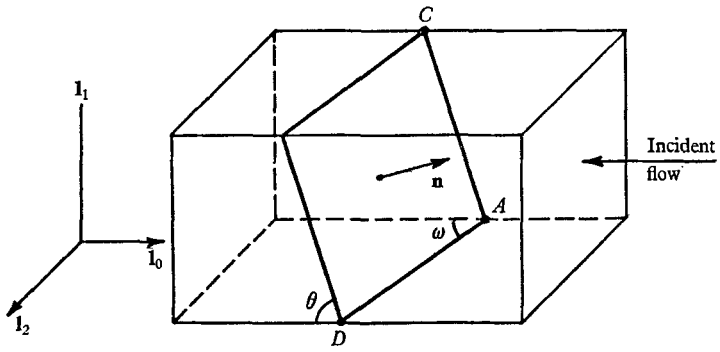

FIGURE 15. Three-dimensional plane detonation wave.

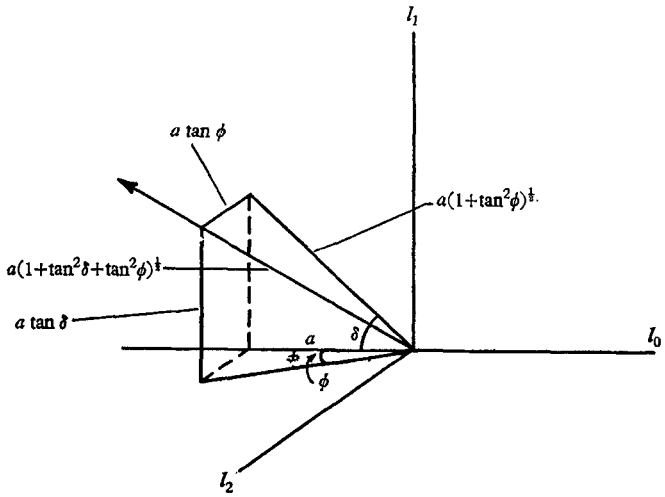

FIGURE 16. Streamline directions behind three-dimensional wave.

In obtaining an expression for the Mach number downstream of the detonation, it was found convenient to show that in the expression for M_1, δ and ϕ only occurred in the form $\tan^2\delta + \tan^2\phi$ and hence was constant around the polar at a given pressure ratio. It may then be shown that

$$M_2^2 = \frac{1}{\dfrac{\gamma_0+1}{\gamma_0-1}+\dfrac{P_1}{P_0}+2q}\left\{\frac{\gamma_0}{\gamma_1}\left(\frac{\gamma_1+1}{\gamma_1-1}+\frac{P_0}{P_1}\right)M_0^2 - \frac{2(P_1/P_0-1)}{\gamma_1(P_1/P_0)(\gamma_1-1)} \times\left[\gamma_1\frac{P_1}{P_0}+q+\frac{\gamma_0(\gamma_1+1)}{\gamma_0-1}\right]\right\}. \tag{A 7}$$

In using the expression for the detonation wave angle θ, (A 6), care must be taken to assign to $\tan\theta$ the sign of δ. Once this is done ω from (A 6) will have the

correct sign. The relations for the normal to the detonation wave are correct in the first quadrant where θ and ω are positive. However, in other quadrants the signs are incorrect and this led the author into many difficulties in a computer program. The requirements are: (i) $\tan\theta\tan\omega/x$ must always be positive to ensure that the wave has the flow approaching from the positive x direction; (ii) $\tan\omega/x$ has the sign of δ and $\tan\theta/x$ has the sign of ϕ.

Appendix B. Rotation matrices for reflected polars

The rotation matrix for the direction cosines of the flow downstream of the incident shock given in appendix A is

$$\begin{bmatrix} \dfrac{1}{(1+x^2)^{\frac{1}{2}}} & \dfrac{x}{(1+x^2)^{\frac{1}{2}}} & 0 \\ \dfrac{-\tan}{(1+x^2)^{\frac{1}{2}}} & \dfrac{\tan}{(1+x^2)^{\frac{1}{2}}} & \dfrac{-\tan}{x} \\ \dfrac{-\tan\phi}{(1+x^2)^{\frac{1}{2}}} & \dfrac{\tan\phi}{x(1+x^2)^{\frac{1}{2}}} & \dfrac{\tan\delta}{x} \end{bmatrix}. \tag{B 1}$$

The application of this gives the direction cosines l, m, n of the vector formed by $\tan\delta_r$ and $\tan\phi_r$. Hence from

$$l = \frac{-1}{(1+x_r)^{\frac{1}{2}}}, \quad m = \frac{\tan\delta_r}{(1+x_r^2)^{\frac{1}{2}}}, \quad n = \frac{\tan\phi_r}{(1+x_r^2)^{\frac{1}{2}}}$$

where $x_r^2 = \tan^2\phi_r + \tan^2\delta_r$, the relations (5) are obtained.

The same rotation matrix applied to the normal to the detonation wave gives

$$\tan\theta_r = \frac{x(|\tan\theta'\tan\omega'| + x\tan\omega'\delta/|\delta|)}{\delta/|\delta|\tan\delta_0\tan\omega' - x|\tan\theta'\tan\omega'|\tan\delta_0 - \tan\phi_0\tan\theta'(1+x^2)^{\frac{1}{2}}\phi/|\phi|},$$

$$\tan\omega_r = \frac{x(|\tan\theta'\tan\omega'| + x\tan\omega'\delta/|\delta|)}{\delta/|\delta|\tan\phi_0\tan\omega' + \phi/|\phi|\tan\theta'\tan\delta_0(1+x^2)^{\frac{1}{2}} - x\tan\phi_0|\tan\theta'\tan\omega'|},$$

where vertical bars indicate absolute values.

REFERENCES

BERNSTEIN, L. 1961 *A.R.C. Reps.* 22619, 22753.

BONE, W. A., FRASER, R. P. & WHEELER, W. H. 1936 *Proc. Roy. Soc.* A **235**, 29.

CAMPBELL, C. & WOODHEAD, D. W. 1928 *J. Chem. Soc.* part II, 2094.

EDWARDS, D. H., PARRY, D. J. & JONES, A. T. 1966 *J. Fluid Mech.* **26**, 321.

FAY, J. A. 1952 *J. Chem. Phys.* **20**, 942.

GLASS, G. P., KISTIAKOWSKY, G. B. & MICHAEL, J. V. 1965 *J. Chem. Phys.* **42**, 608.

GOODERUM, P. V. 1958 *NACA TN* 4243.

GUDERLEY, K. G. 1962 *The Theory of Transonic Flow.* Oxford: Pergamon Press.

HENDERSON, L. F. 1968 *J. Fluid Mech.* **30**, 399.

HENDERSON, L. F. & MACPHERSON, A. K. 1968 *J. Fluid Mech.* **32**, 185.

HOMER, J. B. & KISTIAKOWSKY, G. B. 1967 *J. Chem. Phys.* **46**, 4213.

LIGHTHILL, M. J. 1956 *Surveys in Mechanics.* Cambridge University Press.

MACPHERSON, A. K. 1968*a* *Int. Acad. of Astro. Proceedings, of Int. Colloquium on Gasdynamics of Explosions. Astron. Acta* (in the Press).

MACPHERSON, A. K. 1968*b* *12th Symposium (International) on Combustion* (in the Press).

MITROFANOV, V. V., SUBBOTIN, V. A. & TOPCHIAN, M. E. 1963 *PMTF*, **3**, 45.

OPPENHEIM, A. K. 1965 *Astron. Acta*, **11**, 391.

SCHOTT, G. L. 1965 *Phys. Fluids*, **8**, 850.

SHCHELKIN, K. I. & TROSHIN, Ya. K. 1964 *NASA TTF*-321.

SOLOUKHIN, R. I. 1966 *Comb. & Flame*, **10**, 51.

STREHLOW, R. A. 1964 *AIAA J.* **2**, 908.

VOITSEKHOVSKY, B. V. 1957 *Dokl. Akad. Nauk, SSSR* **114**, 717.

WHITE, D. R. 1963 *Phys. Fluids*, **6**, 1011.

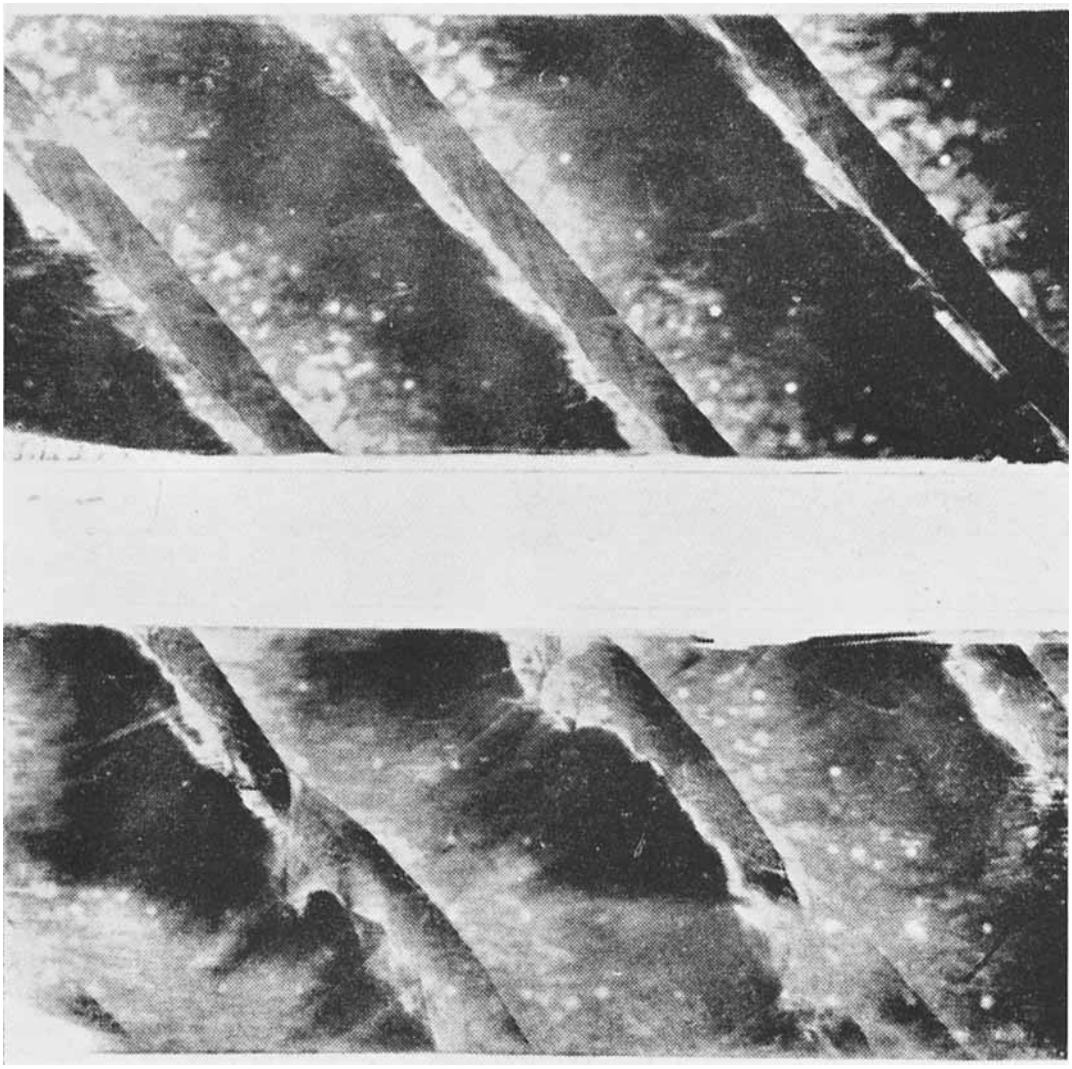

FIGURE 3(*b*). For legend see p. 456.

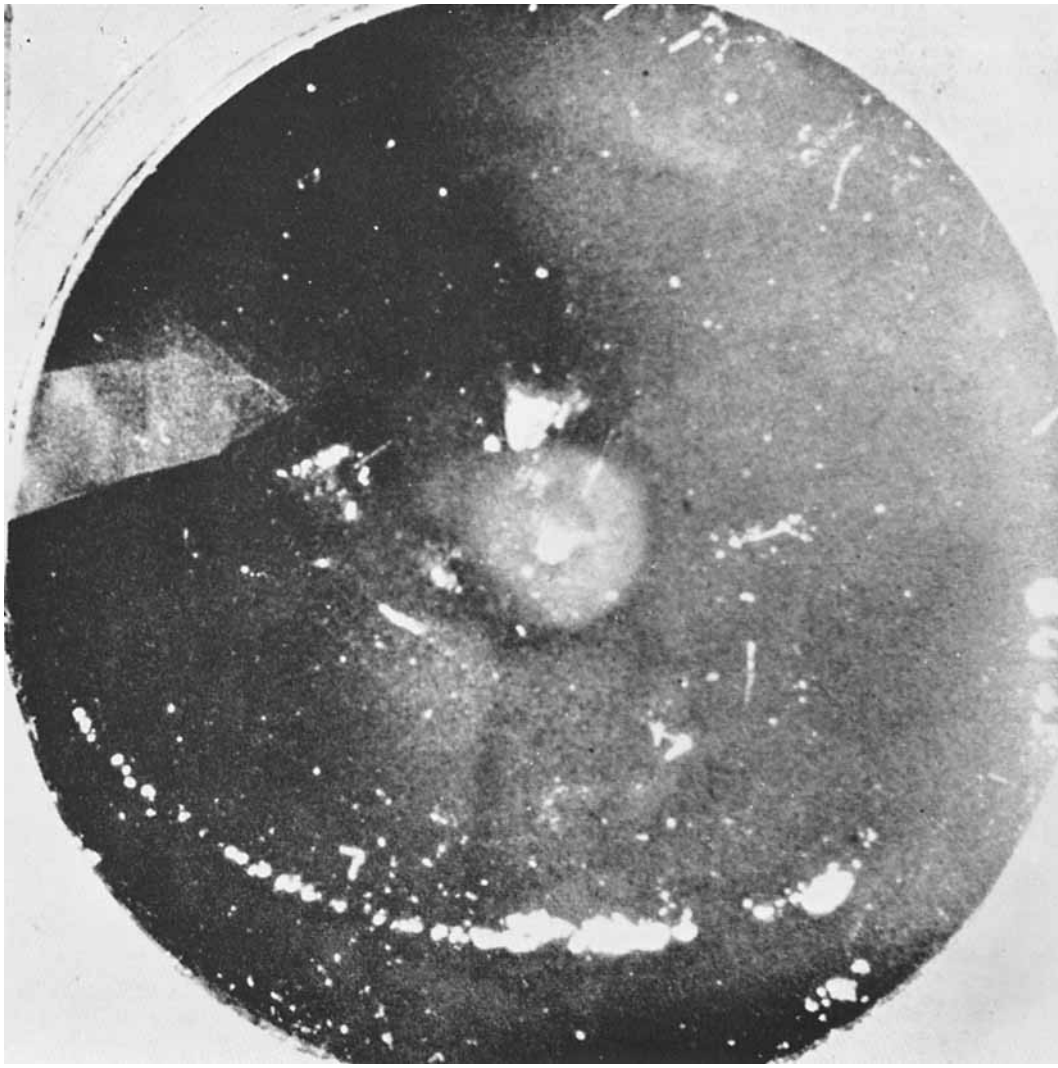

FIGURE 3(*d*). For legend see p. 456.

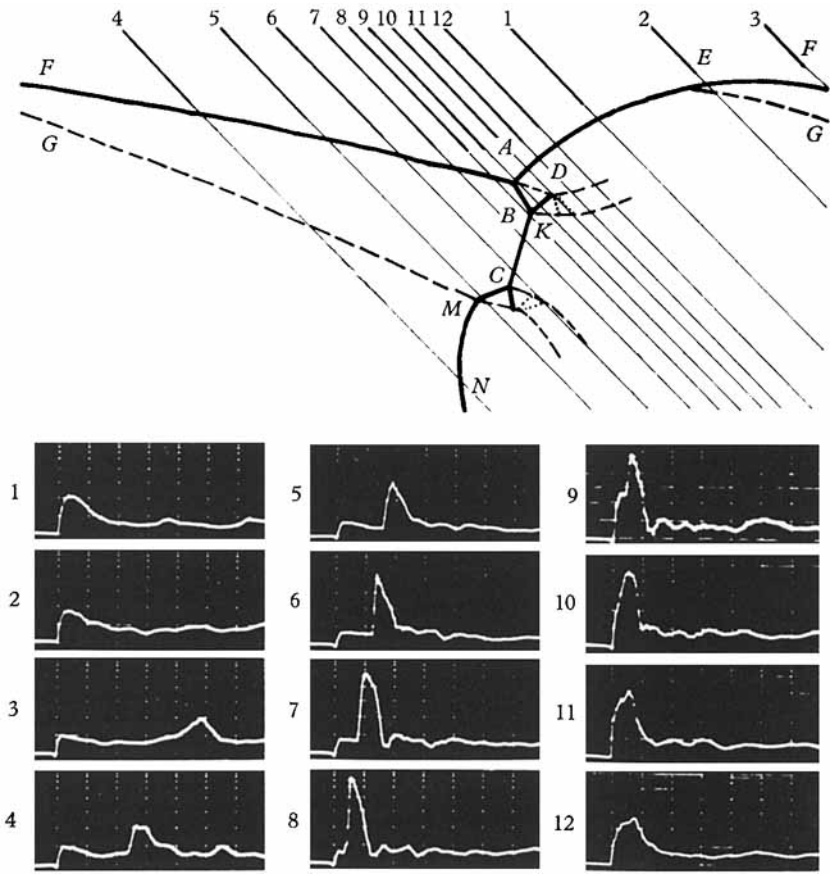

FIGURE 10. Pressure profiles of a spinning detonation and their consequence according to Mitrofanov, Subbotin & Topchian (1963). The experiments were performed with the use of a 2 $CO+O_2+3\%$ H_2 mixture contained in a tube 27 mm in diameter at an initial pressure $p_0 = 0{\cdot}1$ atm. Each division of vertical scale corresponds to $25p_0$, while the horizontal spacing is in 5 μsec intervals.